Piecewise linear differential equations and integrate-and-fire neurons: Insights from two-dimensional membrane models

Arnaud Tonnelier* and Wulfram Gerstner
Laboratory of Computational Neuroscience, EPFL, Lausanne, Switzerland
(Received 10 September 2002; published 19 February 2003)

We derive and study two-dimensional generalizations of integrate-and-fire models which can be found from a piecewise linear idealization of the FitzHugh-Nagumo or Morris-Lecar model. These models give rise to new properties not present in one-dimensional integrate-and-fire models. A detailed analytical study of the models is presented. In particular, (i) for the piecewise linear FitzHugh-Nagumo model, we determine analytically the bistability regime between stationary solutions and oscillations, that is, typical for class-II models. (ii) In the piecewise Morris-Lecar model, we find a noncanonical class-I transition from a stationary state to oscillations with logarithmic dependence similar to that found for leaky integrate-and-fire models. (iii) Furthermore, we establish a relation to the recently proposed resonate-and-fire model and show that a short input current pulse can trigger several spikes.

DOI: 10.1103/PhysRevE.67.021908 PACS number(s): 87.19.La, 87.10.+e, 05.45.−a

I. INTRODUCTION

Neuronal activity is the result of a highly nonlinear dynamic process that was first described mathematically by Hodgkin and Huxley (1952) with a set of four coupled differential equations. Precise descriptions of neuronal activity involve an extensive number of variables and parameters [1,2], which often prevent a clear understanding of the underlying dynamics. Hence, a simplified description of neuronal activity is desirable and has been the subject of numerous works. A pioneering work dates back to Lapicque [3] who proposed a single-variable threshold model for the description of neuronal spike dynamics. Simple models of neuronal activity have become quite popular in neural network modeling [4,5]. Phenomenological descriptions based on a reduction of detailed models has been attempted by many authors using low-dimensional differential equations [6–11]. Facing the lack of standardized descriptions, some authors have proposed a generic description of neuronal activity using concepts of bifurcation theory for dynamical systems [12–14]. Despite the large number of biophysical mechanisms, there are only two majors dynamic mechanisms of excitability for nonbursting cells reported as excitability of class I and II [12,15,16]. Excitable properties of a cell are determined according to the emerging frequency of repetitive firing. Class I is obtained when repetitive action potentials are generated with an arbitrarily low frequency, whereas in class-II action potentials emerge at a nonzero frequency. Typically, class I and II are related to a saddle node on a limit cycle bifurcation and a fold limit cycle bifurcation, respectively.

Most models of neuronal activity use nonautonomous differential equations. Alternatively, integral representations of the cell activity have been formulated [17]. Experimenters typically measure the membrane potential which stands for the observable variable, while it is usually impossible to monitor other dynamic variables, such as gating variables. Therefore, it is valuable to have a direct expression for the membrane potential

$$v(t)=\sum_{t^*\in\mathcal{T}}\eta(t-t^*)+R(t,I(t)), \tag{1}$$

which stands for a generalized version of the spike-response-model [17,18]. Expression (1) allows a clear understanding of the neuronal behavior: the function η is the invariant spike form including the spike afterpotential, the set $\mathcal{T}$ describes the spike events that are to be taken into account, and R models the subthreshold response of the cell to an external input $I(t)$. A spike event occurs if $v(t)$ crosses a threshold ϑ from below. The motivations for the formulation (1) come from the well-known experimental observations that (i) spikes are generated by some type of threshold process and (ii) spikes have an approximately invariant form.

In this paper, we suggest modeling a simple spiking neuron with piecewise linear differential equations. We show that this framework allows a qualitative description of excitable systems through bifurcation analysis but also a quantitative analysis of neuronal behavior through an explicit integral representation of the membrane potential. We mainly focus on two-dimensional membrane models but our analysis can be applied to higher-dimensional systems. Piecewise linear systems are introduced as a first-order approximation of the nonlinear neuronal dynamics. In particular, our models can be derived as a piecewise linear idealization of the FitzHugh-Nagumo model introduced by McKean [19] or as a piecewise linear version of the Morris-Lecar model [8]. At each level, we derive an integral representation equivalent to the differential formulation. We analyze the behavior of these models under an external current $I(t)$ and we emphasize new features not present in one-dimensional integrate-and-fire models. We discuss more specifically two input scenarios (i) a single-short current pulse and (ii) a constant bias current. Our analysis uses the classical tools of differential equation theory but also an equivalent integral formulation.

*Email address: Arnaud.Tonnelier@epfl.ch

We will consider piecewise linear differential equations with a discontinuous right-hand side

$$\frac{dX}{dt} = F(X), \tag{2}$$

where F is expressed as a linear combination of $X \in R^n$ with the Heaviside step function $h(x)$. In order to define precisely a solution of Eq. (2), we need to extend the differential equation to a differential inclusion [20,21]

$$\frac{dX}{dt} \in F(X), \tag{3}$$

where the right-hand side of Eq. (3) is defined with the set-valued Heaviside function

$$h(x) = \begin{cases} \{1\}, & x > 0 \\ [0,1], & x = 0 \\ \{0\}, & x < 0. \end{cases}$$

A solution of Eq. (2) is an absolute continuous function defined on an interval $I \in R$, which satisfies Eq. (3) for almost all $t \in I$. We will mainly use planar systems of piecewise linear differential equations with a line of discontinuity and we refer to Ref. [22] for precise results on the uniqueness for the initial-value problem. In a previous paper, [23], a particularly simple special case of Eq. (3) has been analyzed. Here, we generalize our methods so as to study more realistic piecewise linear approximations of the FitzHugh-Nagumo and Morris-Lecar models. This paper is organized as follows. In Sec. II, we recall the standard integrate-and-fire model and its equivalent integral representation. In Sec. III, we introduce two-dimensional membrane models as a generalization of integrate-and-fire (IF) models including a smooth recovery process. We focus on two particular recovery dynamics that reveal the main qualitative properties of our two-dimensional modeling. We conclude with a discussion.

II. ONE-DIMENSIONAL MODELS OF NEURONAL ACTIVITY

As a starting point, we recall the standard leaky IF model. The IF model is one of the simplest description of the neuronal activity given by a single variable $v(t)$, which stands for the membrane potential. The behavior of the neuron, driven by a current $I(t)$, is given by a linear differential equation

$$\frac{dv(t)}{dt} = -\frac{v(t)}{\tau_1} + c_1 I(t), \tag{4}$$

where $\tau_1 > 0$ is the membrane time constant and c_1^{-1} is a capacity. This model is represented by an RC circuit, where $\tau = (RC)^{-1}$ and $c_1 = C^{-1}$. To keep the mathematical formulation as simple as possible, we take the resting potential of the membrane to be 0. It is obvious that a linear evolution is not a realistic model of neuronal activity. In order to account for spikes one defines the threshold process

$$v(t) = \vartheta \Rightarrow t \in \mathcal{F} \text{ and } v(t^+) = v_r, \tag{5}$$

where $\vartheta > 0$ is the threshold, $\mathcal{F}$ the firing set, v_r the reset value, and $t^+ = \lim_{\epsilon \to 0, \epsilon > 0} t + \epsilon$. In this paper, we assume for simplicity that the firing set is a countable discrete set [i.e., $I(t)$ is bounded and the threshold line is crossed transversely]. In the standard IF model the action potential is not described explicitly and spikes are reduced to formal events $t^f \in \mathcal{F}$, where t^f is the firing time.

Alternatively to the modeling with differential equations one may work with an integral representation of the neuronal activity. For the standard IF model, it is straightforward to derive the integral formulation [17]. Let us suppose that a first spike has occurred at time $\hat{t}^f$. For $t > \hat{t}^f$ the formal result of the integration of Eq. (4) is

$$v(t) = v_r e^{-(t-\hat{t}^f)/\tau_1} + c_1 \int_0^{t-\hat{t}^f} e^{-s/\tau_1} I(t-s)\, ds. \tag{6}$$

Expression (6) is valid up to the moment of the next threshold crossing and when $v(t) = \vartheta$, the integration must restart. The formulation (6) is obtained if the reset condition is introduced as an initial condition. From another point of view, if one treats the reset conditions as a current pulse $I_r(t) = -(\vartheta - v_r)\delta(t - t^f)$ [17], the integration yields

$$v(t) = \sum_{t^f \in \mathcal{F}} -\eta_r(t - t^f) + c_1 \int_0^{\infty} e^{-s/\tau_1} I(t-s)\, ds, \tag{7}$$

where $\eta_r(t) = (\vartheta - v_r) e^{-t/\tau_1}$ if $t > 0$ and 0 otherwise. The firing times $t^f \in \mathcal{F}$ are given by Eq. (5). In contrast to Eq. (6), expression (7) has not to be rewritten when a new firing time is defined. The formulation (7) allows a clear understanding of the IF dynamics; the neuron acts as a convolution filter that emits a reset pulse when the threshold is reached. The convolution is described by the kernel $\epsilon_1(s) = c_1 \exp(-s/\tau_1) h(s)$ and function $\eta_r(s)$ describes the reset pulse related to the reset condition (5). In Fig. 1, we show the voltage $v(t)$ of the standard IF model driven by an input current $I(t)$. Note that the summation in Eq. (7) is not related to an adaptation and one has to emphasize that IF models have no memory beyond the last spike [which is not clear from Eq. (7)].

Let us now consider a simple input scenario which reveals the basic behavior of the standard IF model. We suppose that the IF neuron is stimulated by a constant input current $I(t) = I$. An interesting property is how repetitive firing arises in the system. It is easy to show that the IF neuron fires regularly if the input current is larger than a critical value $I_1 = (c_1 \tau_1)^{-1} \vartheta$. In this case, the firing rate of the IF model is given by

$$\nu = \left(\tau_1 \ln \frac{c_1 \tau_1 I}{c_1 \tau_1 I - \vartheta} \right)^{-1}. \tag{8}$$

Note that the transition is marked by arbitrarily low frequencies and, thus, the excitability is reported as being class I. From Eq. (8), the frequency in the transition to repetitive firing is proportional to $1/\ln(I - I_1)$.

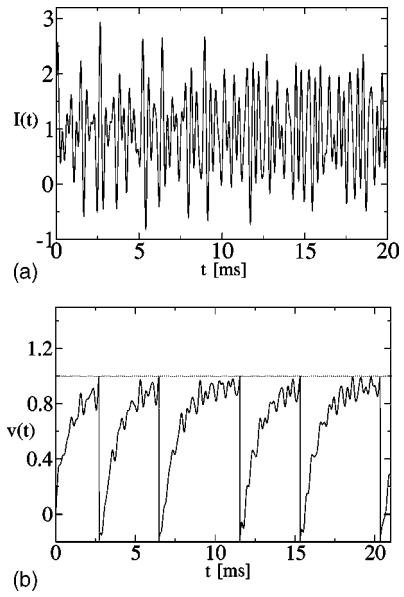

FIG. 1. Voltage $v(t)$ (b) of the standard integrate-and-fire model (4) and (5) driven by the input current $I(t)$ (a). Parameters are $\tau_1=1$, $\vartheta=1$, and $v_r=-0.2$. Input $I(t)$ consists of a superposition of four sinusoidal components plus a positive bias current $I_0=0.94$, which drives the membrane potential towards the threshold.

III. TWO-DIMENSIONAL MODELS

There are two major drawbacks of models based on one-dimensional differential equations: (i) subthreshold oscillations cannot be reproduced and (ii) the reset condition is a nonrealistic recovery process. Firstly, damped oscillations of membrane potential are reported experimentally for many biological neurons [24] and in biophysically detailed neural models [25]. This dynamical property is assumed to play an important role in the neuronal information processing and reveals the sensitivity of neurons to the fine temporal structure of input spike train [26]. Secondly, the reset process in the one-dimensional modeling of neuronal activity is a bad approximation of a biologically realistic smooth recovery process. In this section, we introduce a two-dimensional model which addresses these problems. Let us consider a recovery variable $w(t)\in R$. The two-dimensional system is

$$\frac{dv(t)}{dt}=f(v(t))-w(t)+I_e(t),$$
$$\frac{dw(t)}{dt}=g(v(t),w(t)), \tag{9}$$

where $f(v)$ is the piecewise linear function given by

$$f(v)=-\frac{v}{\tau(v)}+\mu h(v-\vartheta), \tag{10}$$

where $\tau(v)=\tau_1$ if $v<\vartheta$ (subthreshold regime) and $\tau(v)=\tau_2$ otherwise (superthreshold regime). $I_e(t)$ is an effective current, i.e., $I_e(t)=c_1I(t)$ if $v(t)<\vartheta$ and $c_2I(t)$ otherwise.

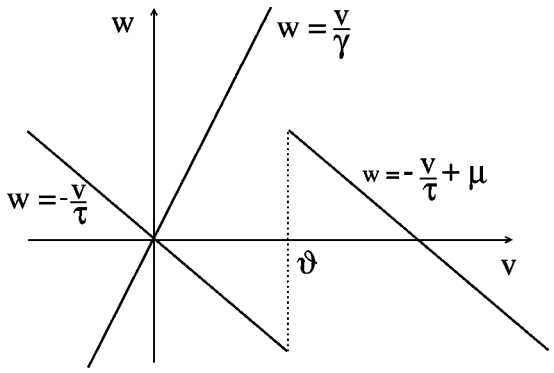

FIG. 2. Nullclines of McKean's model (13) in the monostable case without input, i.e., $I_e(t)=0$.

We will focus on a specific instance of the function g. In the context of piecewise linear differential equation the general form of g is

$$g(v,w)=g_{v,i}v-g_{w,i}w+g_i, \tag{11}$$

where $i=1$ when $v<\vartheta$ and $i=2$ otherwise. In other words g, is a piecewise linear function and we allow for a discontinuity at $v=\vartheta$. Parameters $g_{v,i}$, $g_{w,i}$, and g_2 are positive constants and we take $g_1=0$. The sign of parameters is motivated by the inhibitory role of w and the requirement of a stable resting state at the origin. A complete study of Eqs. (9)–(11) is not the goal of the present work; rather we would like to study some simple configurations that illustrate the qualitative behavior of two-dimensional excitable membrane models. We will emphasize those features of the two-dimensional models that go beyond those of the one-dimensional IF models discussed above. Graphical or geometrical representation of the dynamics in the phase plane is a classical tool for the study of neural excitability and oscillations [12]. Here, our analysis is completed by the analytical description of the neuronal activity through an equivalent integral formulation.

A. The piecewise linear FitzHugh-Nagumo (PFN) model

First, we explore the simple case, where g is the linear function

$$g(v,w)=b(v-\gamma w), \tag{12}$$

where $\gamma\geqslant 0$ and $b>0$. Since we are interested in qualitative properties, we consider for simplicity $\tau_1=\tau_2=\tau$. Hence, we study

$$\frac{dv(t)}{dt}=-\frac{v(t)}{\tau}+\mu h[v(t)-\vartheta]-w(t)+I_e(t),$$
$$\frac{dw(t)}{dt}=b(v-\gamma w). \tag{13}$$

One recognizes the piecewise linear version of the FitzHugh-Nagumo model introduced by McKean [19]. Nullclines of the piecewise linear system (13) are shown in Fig. 2. In Ref. [23], we focused our study on the existence of periodic so-

lutions of Eq. (13) for $\gamma=0$ without input current, i.e., $I_e(t)=0$. In the present study, the w nullcline has a finite positive slope so as to allow the analysis of the phase transition and the bistability with I_e as a bifurcation parameter.

1. Integral formulation of the PFN model

In this section, we show that the two-dimensional model (13) admits an equivalent integral formulation. This representation allows a direct comparison with expressions previously obtained for one-dimensional IF models. Based on the integral formulation, we determine some properties of the neuronal activity.

We define the two sets [27]

$$v(t)=\vartheta \text{ and } \frac{dv}{dt}(t^-)>0\Rightarrow t\in\mathcal{F},$$

$$v(t)=\vartheta \text{ and } \frac{dv}{dt}(t^-)<0\Rightarrow t\in\mathcal{R},$$

where $(dv/dt)(t^-)$ denotes the left-hand side derivative. $\mathcal{F}$ is the firing set analogous to the one that we have already encountered in Sec. II and $\mathcal{R}$ the resetting set. The jump conditions result from the discontinuity of the vector field and indicate that a firing time (a reset time) is defined when the threshold line is crossed from left to right (right to left). We assume that the two sets $\mathcal{F}$ and $\mathcal{R}$ are countable discrete sets. Hence, sliding solutions [20] are not considered in our analysis; some comments are available in the Appendices.

We demonstrate (Appendix A) that the PFN model is equivalent to

$$v(t)=\sum_{t^f\in\mathcal{F}}\eta_f(t-t^f)-\sum_{t^r\in\mathcal{R}}\eta_r(t-t^r)+\int_0^\infty \epsilon(s)I_e(t-s)ds, \tag{14}$$

where $\eta_f(s)$, $\eta_r(s)$, and $\epsilon(s)$ are given in Appendix A. By abuse of notation, we have chosen the same symbols for the IF and PFN kernels. From the Appendix, we have $\eta_f(t)=\eta_r(t)$ and we refer to both kernels simply as $\eta(t)$. We emphasize the existence of a memory effect, i.e., the possibility to emit several spikes in response to a single-short input current $I(t)=q_0\delta(t-t_0)$. This property is related to a memory process caused by the smooth recovery dynamic. We will derive a precise analysis of this PFN feature in the following section.

2. Leaky integrator versus leaky resonator

Depending on the stability of the resting state (stable node or stable focus), the PFN model presents two qualitatively different behaviors, i.e., leaky integrator versus leaky resonator. Such a distinction implies some differences in the neurocomputational properties of neurons [26] and would not be possible for one-dimensional IF models since they always exhibit an exponential convergence to the resting state. In the PFN model, the stability of the resting state is monitored by $\Delta=1/4(1/\tau+\gamma b)^2-b$ (see Appendix A) and depending on its sign the two kernels η and ϵ are expressed with different functions; trigonometric or hyperbolic ones. To make our discussion as clear as possible, we take $\gamma=0$ in Eq. (13). Most of the results are directly generalizable for $\gamma>0$.

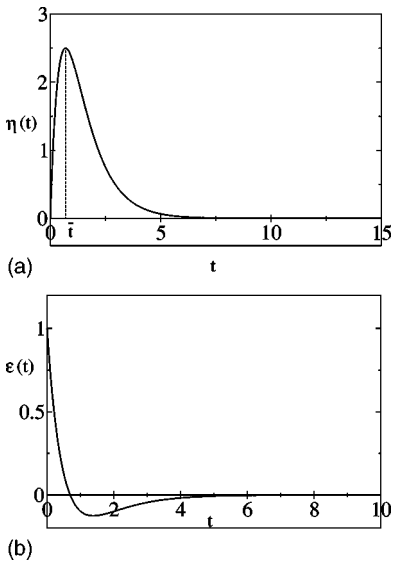

FIG. 3. Kernels of the PFN model in the leaky integrator configuration. (a) shows kernel η and (b) kernel ϵ. Function η has a global maximum at $\bar{t}=1/\omega\,\mathrm{arctanh}2\omega\tau$ and its global minimum is 0. Parameters are $\tau^{-1}=3$, $\mu=10$, and $b=2$.

Leaky integrator. The case $\Delta>0$, i.e., $4b\tau^2<1$, is referred to as the leaky integrator case, and we will explain this terminology later. We set $\omega=1/2\sqrt{1/\tau^2-4b}$ and from Appendix A, we have

$$\eta(t)=\frac{\mu}{\omega}e^{-t/2\tau}\sinh\omega t,$$

$$\epsilon(t)=e^{-t/2\tau}\left(\cosh\omega t-\frac{1}{2\tau\omega}\sinh\omega t\right) \tag{15}$$

for $t>0$ and $\eta(t)=\epsilon(t)=0$ otherwise. The function η has a pulse shape without negative part [Fig. 3(a)]. The term $\epsilon*I$ in Eq. (14) is the response of a convolution filter with impulsive response ϵ. Its typical shape is depicted in Fig. 3(b). Note that $\epsilon(t)$ presents an exponential convergence to the rest state with a short negative bump. Let us remark that this filter is stable, i.e., $\epsilon\in L^1(R)$, and realizable, i.e., $\mathrm{supp}(\epsilon)=R^+$. To understand more closely the sensitivity of the neuron to the input frequency, we calculate the transfer function of the filter $\mathcal{E}$, the Fourier transform of ϵ,

$$\mathcal{E}(\xi)=\frac{2i\pi\xi}{b-4\pi^2\xi^2+2i\pi\dfrac{\xi}{\tau}}. \tag{16}$$

The resonance frequencies are clearly illustrated by the plot of the energy spectrum $|\mathcal{E}(\xi)|^2$ (Fig. 4). High frequencies ($|\xi|$ large) are destroyed and the energy spectrum has a maximum at the frequency

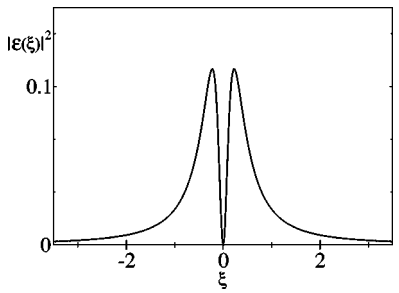

FIG. 4. Spectrum (16) of the subthreshold response of the piecewise linear FitzHugh-Nagumo model. Parameters are $\tau^{-1}=3$ and $b=2$.

$$\xi_p=\frac{\sqrt{b}}{2\pi}, \tag{17}$$

which points out a privileged frequency. The filter gain is zero, i.e., $\mathcal{E}(0)=0$, and thus filter responses have a zero mean value (for $\gamma=0$).

The sensibility to a single-incoming pulse has already been studied in Ref. [23] and will not be repeated here. The main result is that the neuron emits a single spike if $q_0>\vartheta$. Moreover, in the limiting situation $b\to 0$ the behavior is very similar to the one-dimensional IF models (see the discussion) justifying the designation *leaky integrator* [28].

Leaky resonator. We now investigate the other situation, that is, when $4\tau^2 b>1$. We find (Appendix A)

$$\eta(t)=\frac{\mu}{\omega}e^{-t/2\tau}\sin\omega t,$$
$$\epsilon(t)=e^{-t/2\tau}\left(\cos\omega t-\frac{1}{2\tau\omega}\sin\omega t\right) \tag{18}$$

for $t>0$ and $\eta(t)=\epsilon(t)=0$ otherwise. In Eq. (18), we have set $\omega=1/2\sqrt{4b-1/\tau^2}$. The function η has a spike shape that includes an hyperpolarization period [Fig. 5(a)]. The afterpotential is amplified by the resetting pulse $\eta(t-t^r)$. In this configuration, a dynamical threshold that includes the resetting pulse is a reasonable approximation of neuronal activity (see the discussion in the last section). The term $\epsilon * I$ is the response of a convolution filter with an impulse response that shows damped oscillations. The damping is monitored by the parameter τ [Figs. 5(b), and 5(c)]. The filter is still stable and its transfer function is the same (since the transition from the integrator to the resonator states when $\omega=1/2\sqrt{1/\tau^2-4b}$ becomes imaginary). The limiting situation $\tau\gg 1$ is a special case of $4\tau^2 b>0$ and as $\tau\to\infty$, we find

$$\epsilon(t)=\cos\omega_p t+O(1/\tau)$$

for $t>0$, where $\omega_p=\sqrt{b}$. Therefore, for a sinusoidal input $I(t)=\sin\omega_0 t\, h(t)$, we find the leading approximation of the convolution part of the activity

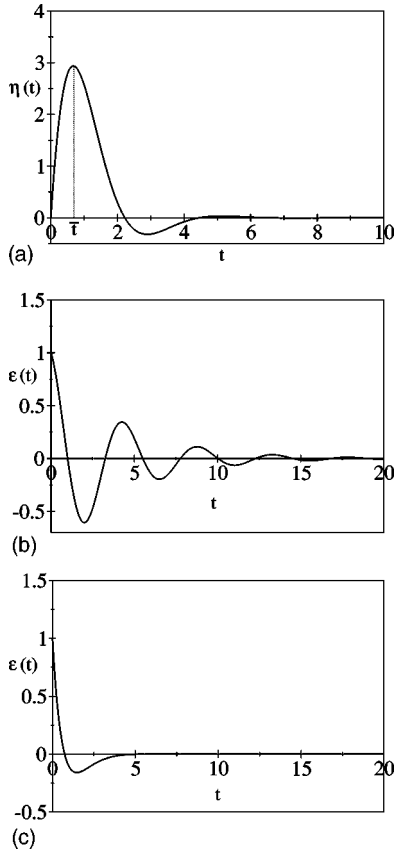

FIG. 5. Kernels of the piecewise linear FitzHugh-Nagumo model in the leaky resonator configuration. (a) Plot of the kernel η for $\tau=0.5$, $\mu=10$, $b=3$. The maximum is reached at $\bar{t}=1/\omega \arctan 2\omega\tau$. The impulsive response ϵ is shown for $b=2$ and $\tau=2$ (b), $\tau=0.4$ (c).

$$\epsilon * I(t)=\begin{cases}\dfrac{\omega_0}{\omega_0^2-\omega_p^2}(\cos\omega_p t-\cos\omega_0 t) & \text{if } \omega_0\neq\omega_p\\ \dfrac{t}{2}\sin\omega_p t & \text{if } \omega_0=\omega_p.\end{cases}$$

For $\omega_0=\omega_p$, a resonating phenomenon occurs which yields an unstable system. This limiting behavior explains the designation *leaky resonator*.

In the leaky resonator case, the neuron prefers periodic inputs of a frequency that is equal to the frequency of the subthreshold oscillations. Moreover, the spike solution is more complex in the sense that a short stimulus $I=q_0\delta(t)$ may elicit a spike train [23]

$$v(t)=\sum_{t^f\in\mathcal{F}}\eta_f(t-t^f)-\sum_{t^r\in\mathcal{R}}\eta_r(t-t^r)+q_0\epsilon(t).$$

The brief current pulse $q_0\delta(t)$ leads to an instantaneous shifting of $v(t)$ from the resting state and the spike solution is a trajectory that spirals around the resting state (see Fig. 6). The number of emitted spikes depends on the proximity of a fold limit cycle bifurcation. The study of this bifurcation is left to the following section.

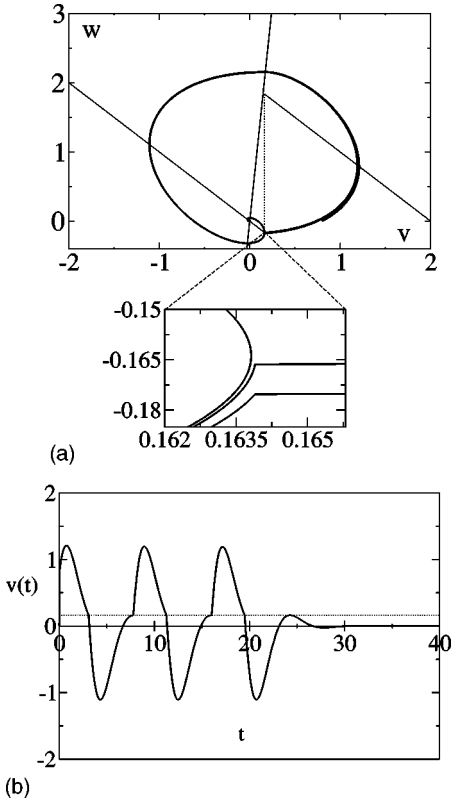

FIG. 6. Spike solution of the piecewise linear FitzHugh-Nagumo model in the leaky resonator case. The neuron is excited from its resting potential by a single-short current pulse $I=q_0\delta(t)$. Panel (a) shows the trajectory in the v-w phase plane. The nullclines are shown in thin lines. The enlarged figure shows the trajectory in the vicinity of the threshold. (b) shows the time course $v(t)$ of the membrane potential. The threshold is shown in thin line. Parameters are $\tau=1$, $\mu=2$, $\vartheta=0.1639$, $b=1$, $\gamma=0.08$, $q_0=0.8$.

3. Constant input and oscillations

In this section, we study some input scenarios that emphasize the major differences between the two-dimensional PFN model and the one-dimensional IF models. We go back to the case $\gamma>0$ in Eq. (12) so that a constant input qualitatively acts on the dynamics by shifting the v nullcline [29]. Before starting the study, we note that the change of variables

$$(\tilde{v},\tilde{w},\tilde{t},\tilde{\vartheta},\tilde{b},\tilde{\gamma},\tilde{I})=\left(\frac{v}{\mu\tau},\frac{w}{\mu},\frac{t}{\tau},\frac{\vartheta}{\mu\tau},\tau^2 b,\frac{\gamma}{\tau},\frac{I}{\mu}\right)$$

allows us to take $\tau=\mu=1$. Recall that the requirement on the threshold is $0<\vartheta<1$. Without external inputs, we avoid an additional stable fixed point in the superthreshold regime fixing γ and ϑ such that

$$\frac{\gamma}{1+\gamma}<\vartheta. \tag{19}$$

In this configuration the spike dynamics, in the superthreshold regime, is driven by the virtual fixed point $[\gamma(1+\gamma)^{-1},(1+\gamma)^{-1}]$. For $\gamma\neq 0$, as the input current I increases, the PFN presents two *nonsmooth* saddle-node bifurcations at $I=I_1$ and I_2, where

$$I_1=\vartheta\left(1+\frac{1}{\gamma}\right)-1,$$

$$I_2=\vartheta\left(1+\frac{1}{\gamma}\right).$$

The nonsmooth term indicates that the saddle point appears or disappears along the line of discontinuity. It is a singular fixed point and a precise mathematical formulation requires the notion of differential inclusions [21].

For $0<I<I_1$ the system has a single stable fixed point, for $I_1<I<I_2$ two stable fixed points and a singular saddle point and for $I>I_2$ a high activity fixed point. We show (Appendix B) that for $I<I_2$ the effect of a constant input current is to decrease the effective threshold following the law

$$\tilde{\vartheta}=\vartheta-\frac{\gamma}{1+\gamma}I.$$

The situation $I>I_2$ is described in the Appendix. Thus, for the analysis of the effects of a constant input, we consider $I=0$. In one-dimensional IF models oscillations are obtained by shifting, through I (or equivalently through ϑ), the low-activity fixed point in the superthreshold region. In the PFN this procedure yields the appearance of a stable fixed point in the superthreshold regime and, therefore, does not involve oscillations. Here, we have to investigate another mechanism for the appearance of oscillations (when they exist).

A periodic solution is related to a periodic configuration of the two sets $\mathcal{F}$ and $\mathcal{R}$. In other words, the existence of a periodic solution is related to the existence of two reals T and ζ such that $t^f=t_{2k}=-\zeta+kT$ and $t^r=t_{2k+1}=\zeta+kT$. Thus, a periodic solution v_∞ is given by

$$v_\infty(t)=\lim_{n\to\infty} v_n(t),$$

where v_n is the spike solution defined from Eq. (14)

$$v_n(t)=\sum_{k=-n}^{n}\eta(t-t_{2k})-\eta(t-t_{2k+1}),$$

where for convenience we rewrite the summation as a symmetric one. Parameter $n\in N$ monitors the number of spikes. We show that (Appendix C)

$$v_\infty(t)=\overline{v_\infty}+\eta_\infty(t+\zeta)-\eta_\infty(t-\zeta),$$

where $\overline{v_\infty}=2\gamma\zeta/[(1+\gamma)T]$ is the mean value of $v_\infty(t)$ and $\eta_\infty(t)$ has an expression given in Appendix C. The existence of periodic solutions is obtained from the matching conditions

$$v_\infty(\zeta)=\vartheta,$$

$$v_\infty(-\zeta)=\vartheta,$$

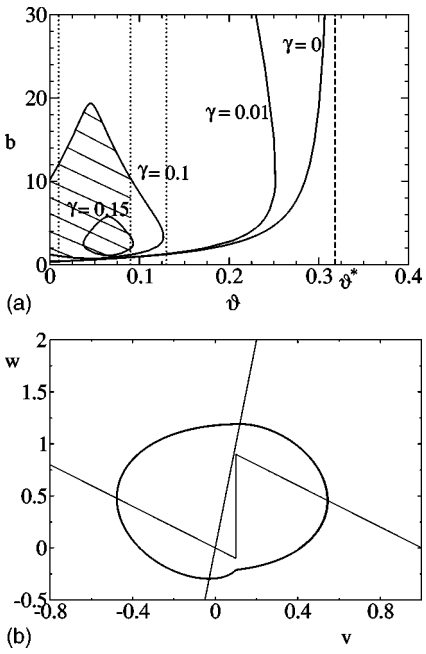

FIG. 7. (a) Locus of existence of periodic solutions (inside the solid lines) for different values of γ. The dotted lines represent the nonsmooth saddle-node bifurcations which yield an additional stable fixed point (to the left side of the line). From left to right, these lines are obtained for $\gamma=0.01$, $\gamma=0.1$, and $\gamma=0.15$. For a value of $\gamma=0.1$, the shaded area indicates the region of the coexistence between a stable limit cycle and two stable fixed points. The long-dashed line represents the critical threshold value ϑ^* above which there is no oscillation. Panel (b) shows in the phase plane the bistable behavior of the piecewise linear FitzHugh-Nagumo model for $\tau=1$, $\mu=1$, $\vartheta=0.1$, $b=2$, and $\gamma=0.1$.

which amounts to the resolution of a system of two transcendental equations (Appendix C)

$$F(x,y)+\frac{\gamma y}{x(1+\gamma)}-\vartheta=0,$$
$$F(x,x-y)-\frac{\gamma y}{x(1+\gamma)}+\vartheta=0, \tag{20}$$

where we write for the notational convenience $x=T/2$ and $y=\zeta$. The existence of periodic solutions is related to the existence of solutions $0<y<x$ of the transcendental system (20). In Fig. 7(a), we depict in the plane (ϑ,b) the locus of existence of periodic solutions for different values of γ. In the terminology of bifurcation theory, the curves [Fig. 7(a)] are fold limit cycle bifurcations [30]. Oscillations appear with a nonzero frequency that indicates a class-II excitability. Figure 7(a) shows a nontrivial dependence of the oscillations upon the threshold. For example, the shaded region gives, for $\gamma=0.1$, the regime of the coexistence between limit cycles and fixed points. The special case $\gamma=0$ has already been analyzed in [23], where an asymptotic value $\vartheta^*=1/\pi$ was found above which no oscillations are possible. Note that for a steady applied current the PFN system still presents a stable fixed point and, thus, when a limit cycle exists, the system presents a bistable behavior [Fig. 7(b)]. A brief current pulse can switch the system from the resting state to the oscillatory response and vice versa. The separatrix between these two regimes is described by an unstable limit cycle. Such behavior has been reported for many models and observed in biological experiments (see Ref. [12]). Moreover, for certain values of (ϑ,b,γ) the system is tristable, that is, there coexists two stable steady states and a stable oscillation. This behavior might be critical for the occurrence of complex bursting behavior.

The advantage of our piecewise linear version of the FitzHugh-Nagumo model is that the problem of the existence of oscillations has been analytically reduced to a solution of transcendental equations which has not been possible in previous works [12].

B. The piecewise linear Morris-Lecar model

The linear evolution (12) of the recovery variable w over the whole phase plane is the simplest dynamic. As for the membrane potential an abrupt evolution of $w(t)$ near the threshold is conceivable. In this case, the recovery function has the form

$$g(v,w)=b[\beta v-\gamma w+\alpha h(v-\vartheta)], \tag{21}$$

where $\alpha>0$. The goal of this section is to illustrate some new aspects of the dynamics induced by the new recovery function (21). When the origin is a focus (necessarily stable because of the sign of parameters) it is possible to obtain oscillations through the same mechanism as in the PFN model; the trajectories spiral ''enough'' around the origin to give rise to a stable limit cycle (for a sufficiently small threshold). In this configuration the model still exhibits class-II excitability. Since we are interested in a new situation, we consider for simplicity $\beta=0$ (the origin is a node) and we will show that this situation give rise to a new behavior. We study the system

$$\frac{dv(t)}{dt}=-\frac{v(t)}{\tau}+\mu h[v(t)-\vartheta]-w+I(t),$$
$$\frac{dw(t)}{dt}=b\{\alpha h[v(t)-\vartheta]-w(t)\}. \tag{22}$$

This system can be obtained as a piecewise linear reduction of the Morris-Lecar model, as we show now.

1. Piecewise linear reduction

The Morris-Lecar equation is a quantitatively accurate model of neurophysiological activity, specifically, the barnacle muscle fiber [8]. The model incorporates two channels: a calcium channel that monitors the spike process and a potassium channel that defines the recovery process. Equations are

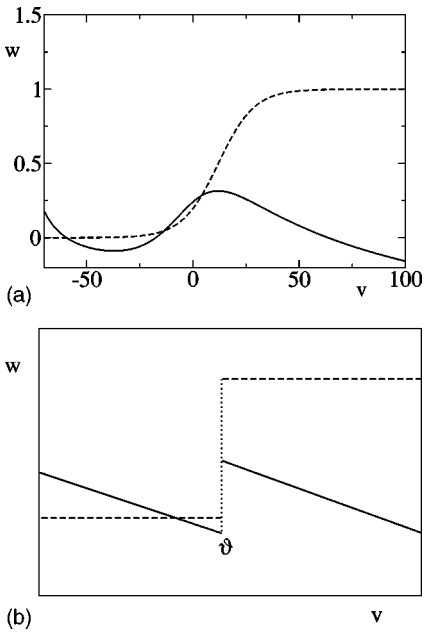

FIG. 8. (a) Nullclines of the Morris-Lecar model and (b) its piecewise linear reduction to a single-threshold system. Parameters in (a) are $V_1=-1.2$, $V_2=18$, $V_3=12$, $V_4=17$, $\bar{g}_{\mathrm{Ca}}=4.4$, $\bar{g}_{\mathrm{K}}=8.0$, $\bar{g}_L=2$, $V_{\mathrm{K}}=-84$, $V_L=-60$, $V_{\mathrm{Ca}}=120$.

$$C\frac{dv}{dt}=\bar{g}_{\mathrm{Ca}}m_\infty(v)(v_{\mathrm{Ca}}-v)+\bar{g}_{\mathrm{K}}w(v_{\mathrm{K}}-v)+\bar{g}_L(v_L-v)+I,$$

$$\frac{dw}{dt}=\epsilon\frac{w_\infty(v)-w}{\tau_w(v)}, \tag{23}$$

where functions $m_\infty(v)$, $w_\infty(v)$, and $\tau_w(v)$ are given in Appendix E. In Eq. (23), v denotes the membrane potential and w is the fraction of open potassium channels. The Morris-Lecar model is more realistic than the FitzHugh-Nagumo model and thus has been increasingly popular for theoretical studies of single cell or network behavior [12,31,32].

The first step of the reduction is obtained by taking the high gain limit for $m_\infty(v)$ and set $m_\infty(v)=h(v-v_1)$. We applied the same procedure to $w_\infty(v)$ and find $w_\infty(v)=h(v-v_3)$. Taking $v_3=v_1=\vartheta$, a constant relaxation time $\tau_w(v)=\tau$ and rescaling ϵ, we obtain

$$\begin{aligned}C\frac{dv}{dt}&=\bar{g}_{\mathrm{Ca}}h(v-\vartheta)(v_{\mathrm{Ca}}-v)+\bar{g}_{\mathrm{K}}w(v_{\mathrm{K}}-v)\\&\quad+\bar{g}_L(v_L-v)+I,\\\frac{dw}{dt}&=\epsilon[h(v-\vartheta)-w].\end{aligned} \tag{24}$$

As a further simplification, we approximate the v nullcline by a piecewise linear function. Rescaling parameters and shifting the resting state to the origin we obtain the piecewise linear system (22) that we call the piecewise linear Morris-Lecar (PML) model. Geometrically, our reduction is sketched in Fig. 8.

2. Integral formulation of the PML

As for the PFN model, we introduce the two sets $\mathcal{F}$ and $\mathcal{R}$. The integral formulation of the PML is given by (Appendix F)

$$v(t)=\sum_{t^f\in\mathcal{F}}\eta_f(t-t^f)-\sum_{t^r\in\mathcal{R}}\eta_r(t-t^r)+\int_0^\infty\epsilon(s)I(t-s)ds, \tag{25}$$

where

$$\epsilon(t)=e^{-t/\tau}$$

and η_f, η_r are given in Appendix F. Using the integral formulation of the PML model (25), an analysis similar to that for the PFN model can be performed. The kernel $\epsilon(t)$ is the same as that of the IF model and hence, the PML neuron is termed leaky integrator. A simple description of the spike η is obtained in the limiting situation $b\to 0$. A fast phase given by

$$\eta(t)=\mu\tau(1-e^{-t/\tau})$$

is followed by a slow phase

$$\eta(t)=\tau(\mu-\alpha)+\alpha\tau e^{-bt}.$$

Note that our analysis concerns a particular reduction of the Morris-Lecar model for which the subthreshold regime has a very simple dynamic. This special choice reveals a great similarity with one-dimensional IF models. We will demonstrate that this similarity also exists in the birth of oscillations.

3. Constant input and oscillations

Just as for the PFN equations, a change of variables allows us to take $\mu=\tau=1$. Without input current, we avoid an additional fixed point in the superthreshold regime if

$$\alpha>1-\vartheta$$

and we still have the requirement on the threshold $0<\vartheta<1$. Depending on the input strength, different fixed points exist. As I increases, two nonsmooth saddle-node bifurcations appear at

$$I=\vartheta=I_1,$$

$$I=I_1+\alpha-1=I_2.$$

For $I<I_1$, one may demonstrate that $(I,0)$ is a globally attractive fixed point. Due to the stability of the fixed point (negative real eigenvalues of the Jacobian matrix) a fold limit cycle bifurcation cannot occur since the trajectory cannot spiral around it. In this regime, the qualitative effect of a constant input is to decrease the threshold value of the isolated system. For $I_1<I<I_2$, the system can be rewritten as a piecewise linear version of a Liénard equation for which a limit cycle exists. The periodic solution is given by (Appendix G)

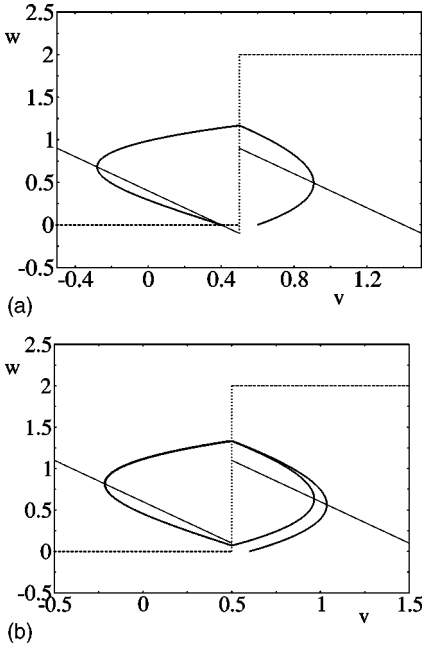

FIG. 9. Trajectory of the piecewise linear Morris-Lecar model for a constant current (a) $I=0.4$ and (b) $I=0.6$. Initial conditions are $(v_0,w_0)=(0.6,0)$ and parameters are $\tau=1$, $\vartheta=0.5$, $\mu=1$, $b=0.3$, $\alpha=2$. In panel (a) the input current is below the saddle-node bifurcation ($I<I_1$) and the resting state is globally attractive. Panel (b) shows the onset of repetitive firing.

$$v_\infty(t)=\overline{v_\infty}+\eta_\infty(t+\zeta)-\eta_\infty(t-\zeta),$$

where $\overline{v_\infty}=2\zeta/T(1-\alpha)+I$ and η_∞ is given in Appendix G. By abuse of notation, we do not distinguish with the notations for the PFN and the PML model. The two unknowns $T=2x$ and $\zeta=y$ are solutions of the transcendental system

$$I-I_1+F(x,y)=0,$$

$$I_2-I+F(x,x-y)=0,$$

monitored by the distance of I to the two bifurcations points I_1 and I_2. For $I>I_2$ the limit cycle disappears via a saddle node on a limit cycle and the new fixed point $(\alpha-1-I,\alpha)$ is globally attractive. Note that there is no bistable behavior (Fig. 9).

The transition to repetitive firing is marked by arbitrarily low frequencies and the model presents a class-I excitability. More precisely, for I near the critical current the frequency is proportional to $1/\ln|I-I^*|$ ($I^*=I_1$ or $I^*=I_2$) as for the integrate-and-fire model (Appendix G) (see Fig. 10). When $I=I^*$ the limit cycle has an infinite period, it is a saddle node on a limit cycle bifurcation. The PML model presents a *noncanonical* transition in the sense that the repetitive firing does not follow the classical $\sqrt{I-I^*}$ law obtained in the smooth case [33]. Note that the logarithmic law is obtained in smooth dynamical system when the limit cycle appears via a saddle loop [33].

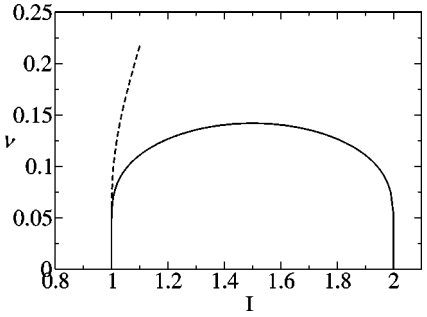

FIG. 10. Frequency $\nu(I)$ of repetitive firing as a function of current for the (class-I) piecewise linear Morris-Lecar model. The dashed line shows the logarithmic law near the first critical current I_1; $\nu(I)\sim -1/b\ln(I-I_1)$. Parameters are $\tau=1$, $\mu=1$, $\vartheta=1$, $b=0.5$, and $\alpha=2$. Hence, the value of the two critical currents is $I_1=1$ and $I_2=2$, respectively.

IV. DISCUSSION

Two-dimensional differential equations are often seen as a useful compromise for a more realistic modeling of the neuronal activity; systems with less than two dimensions incorporate some unrealistic reset behaviors and do not reveal all the excitable properties of neurons. Higher-dimensional systems are difficult to analyze and often do not present significant novel effects. Two-dimensional models of neuronal activity have been widely used and studied [6–10,12]. In this paper, we present two-dimensional systems in the framework of piecewise linear differential equations. Classically, piecewise linear systems have been introduced as an idealization of smooth nonlinearities in order to analyze and to discuss aspects of neural dynamics [19,34,35].

Alternatively, our equations may be introduced as a generalization of the leaky integrate-and-fire model with the aim to define the simplest nonlinear dynamics. The relation between the standard IF model and the two-dimensional models is clearly illustrated by introducing a one-dimensional IF model with a spike description (IFS)

$$\frac{dv(t)}{dt}=-\frac{v(t)}{\tau}+\mu h[v(t)-\vartheta]+I_e(t), \tag{26}$$

where the positive constant μ drives the spike towards a stable fixed point $v_s=\tau_2\mu\gg\vartheta$. This equation is formally equivalent to the v dynamics in Eqs. (13) and (22) of two-dimensional models. However, instead of a smooth recovery process via the dynamics of a recovery variable w, we simply define a reset process when the potential reaches a given superthreshold value ϑ^{peak}, that is,

$$v(t)=\vartheta^{\text{peak}}\Rightarrow v(t^+)=v_r, \tag{27}$$

where $\vartheta<\vartheta^{\text{peak}}<v_s$. Models (26) and (27) is a natural generalization of the standard IF model; the subthreshold and the superthreshold dynamics are both described by RC circuits (for simplicity, we keep the same relaxation constant in the subthreshold and superthreshold regime). The superthreshold regime has an intrinsic drift monitored by μ and a reset condition control by ϑ^{peak}. We could, for example, relate the

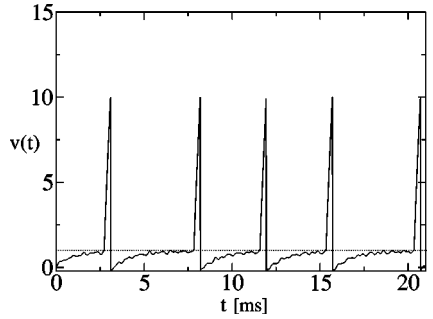

FIG. 11. Voltage $v(t)$ of the integrate-and-fire model with a spike-description driven by the input current $I(t)$ shown in Fig. 1(a). Parameters in the subthreshold regime are the same as Fig. 1 and for the superthreshold regime parameters are $\tau_2=1$, $\vartheta^{\text{peak}}=10$, and $\mu=30$.

superthreshold drift μ to the sodium current of the Hodgkin-Huxley model and v_s to the sodium equilibrium potential. In Appendix H1, we give the integral representation of the IFS model and emphasize the differences with the standard IF model. We present in Fig. 11 the time course of the IFS model for the same input as in Fig. 1. In the same Appendix, we also show that our two-dimensional piecewise linear models have, in the limit of a slow recovery $b\to 0$, a fast regime with nearly identical kernels as the IFS models.

Another point of view is to consider neurons as ''bimodal'' systems defined by two different linear behaviors, i.e., subthreshold and superthreshold dynamics. The main assumption for this modeling is to consider neurons to operate in two modes with a transition from one mode to the other that is taken as instantaneous. In other words, the time scale of the transition is much smaller than the scale of the dynamics of individual modes.

The geometrical treatment of low-dimensional models allows to see more clearly the underlying qualitative structure of models [12]. However, a deep understanding needs the addition of some analytic methods or analytic descriptions of solutions. Our approach provides an exact correspondence with the integral representation of neuronal activity given by

$$v(t)=\sum_{t^f\in\mathcal{F}}\eta_f(t-t^f)-\sum_{t^r\in\mathcal{R}}\eta_r(t-t^r)+\int_0^\infty \epsilon(s)I(t-s)ds, \tag{28}$$

where the kernels η_f, η_r, and ϵ characterize the spike process and the spike generation. The sets $\mathcal{F}$ and $\mathcal{R}$ describe the transitions between the two regimes of the neuron. Note that Eq. (28) can be introduced independently as a model for the neuronal activity assuming that (i) neurons behave as threshold elements that fire when the voltage membrane reaches a threshold, (ii) the spike has an invariant shape, and (iii) the subthreshold part of the dynamics is well approximated by a linear evolution.

It is obvious that Eq. (28) presents an analogy with the standard form of the spike-response-model

$$v(t)=\eta(t-\hat{t}^f)+\int_0^\infty \epsilon(s)I(t-s)ds, \tag{29}$$

where $\hat{t}^f$ is the most recent firing time. However, some reductions or approximations have to be made in order to derive Eq. (29) from Eq. (28). Basically, these transformations follow two steps: (i) reduction of the two η summations into one and (ii) reduction of the single summation into a single term. One possible approach is to assume a constant spike duration $\delta=t^f-t^r$, where t^f and t^r are two related firing and reset time and $\delta>0$ satisfies $\eta(\delta)=\vartheta$. This approximation is useful if we assume that the input is shunted in the superthreshold regime. In this case, the effective current is given by

$$I_e(t)=\rho_{\mathcal{F}}(t)I(t), \tag{30}$$

where $\rho_{\mathcal{F}}$ is the cutoff function

$$\rho_{\mathcal{F}}(t)=1-\sum_{t^f\in\mathcal{F}}\chi_{[t^f,t^f+\delta]}(t).$$

Since the reset time t^r is directly obtained from the firing time t^f, the two summations are reduced into one summation of $\tilde{\eta}(t)=\eta_f(t)-\eta_r(t-\delta)$. Usually $\tilde{\eta}(t)$ has an exponential decay so that we approximate the single summation by its most recent term and we obtain Eq. (29).

It has been shown that Eq. (29) provides an accurate description of some conductance-based models [36]. Here, we have shown that the integral representation (28) can be obtained analytically from two-variable simplifications of detailed conductance-based models. These simplifications are the piecewise linear versions of the FitzHugh-Nagumo model and the Morris-Lecar model. Based on this formulation, we have shown that integrator models have a typical kernel given by

$$\epsilon(t)=e^{-t/\tau}.$$

Popular examples are the integrate-and-fire model and the piecewise linear version of the class-I Morris-Lecar model. Resonator models with damped oscillations have a kernel given by

$$\epsilon(t)=e^{-t/\tau}\cos\omega t.$$

A typical example is the FitzHugh-Nagumo model. There is also an interesting relation to resonate-and-fire models [26]. In addition, the superthreshold process is described by the kernel η. Like the kernel ϵ, this kernel presents to qualitatively different shapes which yield two different laws for the frequency of the emerging oscillations. A kernel η without damped oscillation yields an emerging frequency proportional to $1/|\ln(I-I^*)|$, where I^* is the value of the critical current. This case is refered as class-I neural excitability. For a kernel η with damped oscillations, the model has a class-II neural excitability and presents a nontrivial emerging frequency. The mathematical analysis of class II yields nontrivial conditions for the existence of oscillations, while oscillations in class-I models are easily described from the analysis of the saddle-node bifurcation.

ACKNOWLEDGMENT

The authors thank Magnus Richardson for many valuable suggestions.

APPENDIX A: THE INTEGRAL FORMULATION OF THE PFN MODEL

Let us recall the PFN equations

$$\frac{dv(t)}{dt} = -\frac{v(t)}{\tau} + \mu h[v(t)-\vartheta] - w(t) + I(t),$$
$$\frac{dw(t)}{dt} = b[v(t)-\gamma w(t)]. \tag{A1}$$

For convenience, we write I rather than I_e. We start by transforming (A1) into a linear nonautonomous differential equation using

$$h[v(t)-\vartheta] = \sum_{t^f\in\mathcal{F}} h(t-t^f) - \sum_{t^r\in\mathcal{R}} h(t-t^r), \tag{A2}$$

and thus, (A1) can be solve using classical integral transform methods. Note that (A2) holds for noncontinuous threshold crossing. As an initial condition, we take $(v(0),w(0)) = (0,0)$. Applying the Laplace transform

$$\mathcal{L}(v)(p) = \int_0^\infty e^{-ps} v(s)\,ds,$$

yields

$$p\mathcal{L}(v)(p) = -\frac{1}{\tau}\mathcal{L}(v)(p) + \frac{\mu}{p}\sum_{t^f\in\mathcal{F}} e^{-pt^f} - \frac{\mu}{p}\sum_{t^r\in\mathcal{R}} e^{-pt^r} - \mathcal{L}(w)(p) + \mathcal{L}(I)(p),$$
$$p\mathcal{L}(w)(p) = b[\mathcal{L}(v)(p) - \gamma\mathcal{L}(w)(p)].$$

Thus, we obtain

$$\mathcal{L}(v)(p) = \frac{\mu(p+b\gamma)}{p\left[p^2+\left(b\gamma+\frac{1}{\tau}\right)p+b\left(1+\frac{\gamma}{\tau}\right)\right]} \times\left(\sum_{t^f\in\mathcal{F}} e^{-pt^f} - \sum_{t^r\in\mathcal{R}} e^{-pt^r}\right) + \frac{p+b\gamma}{p^2+\left(b\gamma+\frac{1}{\tau}\right)p+b\left(1+\frac{\gamma}{\tau}\right)}\mathcal{L}(I)(p).$$

We define

$$2s = \frac{1}{\tau} + \gamma b,$$

$$4\Delta = \left(\frac{1}{\tau} - b\gamma\right)^2 - 4b.$$

We do not investigate the case $\Delta = 0$, which yields distinct calculations but does not present a particular interest. Using inverse Laplace transform, the following properties:

$$\mathcal{L}^{-1}[F(p)e^{-pt_i}](t) = \mathcal{L}^{-1}[F(p)](t)h(t-t_i),$$
$$\mathcal{L}^{-1}(FG) = \mathcal{L}^{-1}(F) * \mathcal{L}^{-1}(G),$$

and the formula (for $r_1 \neq r_2$)

$$\mathcal{L}^{-1}\left(\frac{1}{(p-r_1)(p-r_2)}\right)(t) = \frac{1}{r_1-r_2}(e^{r_1 t} - e^{r_2 t}),$$
$$\mathcal{L}^{-1}\left(\frac{1}{p(p-r_1)(p-r_2)}\right)(t) = \frac{1}{r_1 r_2} + \frac{e^{r_1 t}}{r_1(r_1-r_2)} + \frac{e^{r_2 t}}{r_2(r_1-r_2)},$$

we calculate

$$v(t) = \sum_{t^f\in\mathcal{F}} \eta(t-t^f) - \sum_{t^r\in\mathcal{R}} \eta(t-t^r) + \int_0^\infty \epsilon(s) I(t-s)\,ds,$$

where

$$\eta(t) = \frac{\gamma\mu\tau}{\tau+\gamma} + \mu e^{-st}\left[\frac{1}{\sqrt{\Delta}}\left(1 - \frac{s\gamma\tau}{\tau+\gamma}\right)\sinh\sqrt{\Delta}t - \frac{\gamma\tau}{\tau+\gamma}\cosh\sqrt{\Delta}t\right] \tag{A3}$$

for $t>0$ and 0 otherwise. The convolution part of the activity is described by the kernel

$$\epsilon(t) = e^{-st}\left(\cosh\sqrt{\Delta}t + \frac{1}{\sqrt{\Delta}}(b\gamma - s)\sinh\sqrt{\Delta}t\right)$$

for $t>0$ and 0 otherwise, where the parameter $\sqrt{\Delta}$ varies in the complex plane. Depending on the sign of Δ [related to the stability of the resting state (0,0)], we obtain hyperbolic or trigonometric functions. Note that $\gamma\mu\tau/(\tau+\gamma)$ represents the possible fixed point in the superthreshold regime.

APPENDIX B: THE PFN MODEL WITH CONSTANT INPUT

For $I<I_2$, we define

$$v_0 = \frac{\gamma I}{1+\gamma},$$

$$w_0 = \frac{I}{1+\gamma},$$

which is a stable fixed point of the PFN model (as long as $I<I_2$). We consider the change of variables $\tilde{v}=v-v_0$ and $\tilde{w}=w-w_0$. Then the PFN equations rewrite

$$\frac{d\tilde{v}(t)}{dt}=-\tilde{v}+h(\tilde{v}+v_0-\vartheta)-\tilde{w},$$

$$\frac{d\tilde{w}(t)}{dt}=b(\tilde{v}-\gamma\tilde{w}).$$

Introducing the new threshold $\tilde{\vartheta}=\vartheta-v_0$, we find the isolated PFN system. Note that we still have a positive threshold value $\tilde{\vartheta}>0$.

For $I>I_2$, we note

$$v_1=\gamma\frac{I+1}{1+\gamma},$$

$$w_1=\frac{I+1}{1+\gamma},$$

and we consider the change of variables $\tilde{v}=v_1-v$ and $\tilde{w}=w_1-w$. Using $h(x)=1-h(-x)$, we have

$$\frac{d\tilde{v}(t)}{dt}=-\tilde{v}+h(\vartheta+\tilde{v}-v_1)-\tilde{w},$$

$$\frac{d\tilde{w}(t)}{dt}=b(\tilde{v}-\gamma\tilde{w}),$$

and considering $\tilde{\vartheta}=v_1-\vartheta$, we find the isolated PFN system.

APPENDIX C: PERIODIC SOLUTIONS OF THE PFN MODEL

We consider the spike solution in the leaky resonator case (the leaky integrator neuron can only emit a single spike)

$$v(t)=\sum_{t^f\in\mathcal{F}}\eta(t-t^f)-\sum_{t^r\in\mathcal{R}}\eta(t-t^r)+q_0\epsilon(t).$$

We are interested on periodic solutions and, therefore, we do not consider the transient regime monitored by q_0. A periodic solution is obtained as the limit of the spike solution for an infinite number of regular interspike intervals, which reads

$$v_\infty(t)=\lim_{n\to\infty}\sum_{k=-n}^{n}\eta(t-kT+\zeta)-\eta(t-kT-\zeta),$$

where we use the notations previously introduced. We note [see Eq. (A3)]

$$\eta(t)=\frac{\gamma}{1+\gamma}h(t)+\tilde{\eta}(t),$$

and formal calculations lead to

$$v_\infty(t)=\frac{\gamma}{1+\gamma}\sum_{k=-\infty}^{\infty}h(t-kT+\zeta)-h(t-kT-\zeta)+\sum_{k=-\infty}^{\infty}\tilde{\eta}(t-kT+\zeta)-\tilde{\eta}(t-kT-\zeta),\qquad\text{(C1)}$$

that we write

$$v_\infty(t)=v_\infty^a(t)+v_\infty^b(t).$$

The first term $v_\infty^a(t)$ reads

$$v_\infty^a(t)=\sum S_{kT}\chi_{[-\zeta,\zeta]}(t),$$

where χ is the indicatrix function and S the shift operator. This is a T-periodic function such that

$$v_\infty^a(t)=\frac{\gamma}{1+\gamma}\chi_{[-\zeta,\zeta]}(t)\quad\text{on}\quad[-T/2,T/2],$$

which has a Fourier series expansion given by

$$v_\infty^a(t)=\overline{v_\infty}+\frac{\gamma}{1+\gamma}\sum_{k\neq0}\frac{e^{2i\pi k\zeta}-e^{-2i\pi k\zeta}}{2i\pi k}e^{2i\pi kt/T},$$

where we note $\overline{v_\infty}=2\zeta\gamma/[T(1+\gamma)]$. We have $\tilde{\eta}\in L^1(R)$ and then the Poisson formula gives

$$v_\infty^b(t)=\frac{1}{T}\sum_{k=-\infty}^{+\infty}\hat{\tilde{\eta}}(k/T)(e^{2i\pi kt+\zeta/T}-e^{2i\pi k\,t-\zeta/T}).$$

From Eq. (A3) (written with trigonometric functions since $\Delta<0$), we calculate

$$\hat{\tilde{\eta}}(\xi)=\left(1-\frac{s\gamma}{1+\gamma}\right)\frac{1}{-4\pi^2\xi^2+2i\pi(1+b\gamma)\xi+b(1+\gamma)}-\frac{\gamma}{2(1+\gamma)}\frac{1+\gamma b+4i\pi\xi}{-4\pi^2\xi^2+2i\pi(1+b\gamma)\xi+b(1+\gamma)},$$

and then we rearrange v_∞^a and v_∞^b into

$$v_\infty(t)=\overline{v_\infty}+\eta_\infty(t+\zeta)-\eta_\infty(t-\zeta),\qquad\text{(C2)}$$

where η_∞ has a Fourier series expansion

$$\eta_\infty(t)=\sum_n\eta_{\infty,k}e^{2i\pi kt/T},$$

such that

$$\eta_{\infty,k}=\frac{1}{T}\frac{b\gamma+\dfrac{2i\pi k}{T}}{\dfrac{2i\pi k}{T}\left[-\dfrac{4\pi^2k^2}{T^2}+\dfrac{2i\pi k}{T}(1+b\gamma)+b(1+\gamma)\right]}. \tag{C3}$$

Note that the Fourier coefficient of v_∞ is given by

$$v_{\infty,k}=\eta_{\infty,k}(e^{2i\pi k\zeta/T}-e^{-2i\pi k\zeta/T}).$$

Alternatively, one can find this result using the Fourier series transform on the differential formulation of the PFN. Now let us analytically derive the expression of $\eta_\infty(t)$. Starting from (C3), we split the fraction into simple elements and we use the two formula

$$\sum_k \frac{e^{ikt}}{k-ic}=\frac{i\pi}{\sinh(\pi c)}e^{c(\pi-t)} \quad \text{for} \quad t\in[0,2\pi],$$

with $c\in R^*$ and

$$\sum_{k>0}\frac{1}{k}\sin kt=\frac{1}{2}(\pi-t) \quad \text{for} \quad t\in[0,2\pi].$$

We obtain (details not shown)

$$\begin{aligned}\eta_\infty(t)=&\frac{\gamma}{1+\gamma}\left(\frac{1}{2}-\frac{t}{T}\right)\\&+\frac{1}{2r(\cosh sT-\cos rT)}\{e^{-st}[c_1\sin r(T-t)\\&-c_2\cos r(T-t)]+e^{s(T-t)}[c_1\sin rt+c_2\cos rt]\}\end{aligned}$$

for $t\in[0,T]$, where $r=\sqrt{-\Delta}$, $c_1=1+s\gamma/(1+\gamma)$ and $c_2=r\gamma/(1+\gamma)$. Function $\eta_\infty(t)$ is defined on R by periodicity. Conversely, by construction the solution given by Eq. (C2) is a periodic solution of PFN.

Note that our analysis captures periodic solutions that cross $v=\vartheta$ two times (over one period). Periodic solutions that remain on the line of discontinuity over a nonempty time interval are sliding motion solutions [20] and are not characterized by our analysis (because of the definition of t^f and t^r). In our system, periodic solutions with sliding motions are unstable and appear with a bigger stable periodic solution without a sliding motion. Therefore, stable solutions are still detected by our analysis.

APPENDIX D: EXISTENCE OF PERIODIC SOLUTIONS OF THE PFN EQUATIONS

We note $x=T/2$ and $y=\zeta$. The existence of periodic solutions is related to the existence of x and y such that

$$\begin{aligned}&v_\infty(y)=\vartheta,\\&v_\infty(-y)=\vartheta,\end{aligned}$$

which reads

$$\begin{aligned}&\eta_\infty(2y)-\eta_\infty(0)+\frac{\gamma y}{(1+\gamma)x}-\vartheta=0,\\&\eta_\infty(0)-\eta_\infty(-2y)+\frac{\gamma y}{(1+\gamma)x}-\vartheta=0.\end{aligned} \tag{D1}$$

From $\eta_\infty(-2y)=\eta_\infty[2(x-y)]$, we write (D1) as

$$F(x,y)=\vartheta-\frac{\gamma y}{(1+\gamma)x},$$

$$F(x,x-y)=-\vartheta+\frac{\gamma y}{(1+\gamma)x},$$

where $F(x,y)=\eta_\infty(2y)-\eta_\infty(0)$.

APPENDIX E: THE MORRIS-LECAR MODEL

The differential equations are

$$C\frac{dv}{dt}=\bar{g}_{\mathrm{Ca}}m_\infty(v)(v_{\mathrm{Ca}}-v)+\bar{g}_{\mathrm{K}}w(v_{\mathrm{K}}-v)+\bar{g}_L(v_L-v)+I,$$

$$\frac{dw}{dt}=\epsilon\frac{w_\infty(v)-w}{\tau_w(v)},$$

where the v-dependent functions are

$$m_\infty(v)=\frac{1}{2}\left(1+\tanh\frac{v-v_1}{v_2}\right),$$

$$w_\infty(v)=\frac{1}{2}\left(1+\tanh\frac{v-v_3}{v_4}\right),$$

and

$$\tau_\infty(v)=\frac{1}{\cosh\dfrac{v-v_3}{2v_4}}.$$

APPENDIX F: THE INTEGRAL FORMULATION OF THE PML MODEL

As for the PFN model, we transform the PML equations into a nonautonomous linear differential system. Applying the Laplace transform, we find

$$\begin{aligned}p\mathcal{L}(v)(p)=&-\frac{\mathcal{L}(v)(p)}{\tau}+\frac{\mu}{p}\left(\sum_{t^f\in\mathcal{F}}e^{-pt^f}-\sum_{t^r\in\mathcal{R}}e^{-pt^r}\right)\\&+\mathcal{L}(I)(p),\end{aligned}$$

$$p\mathcal{L}(w)(p)=-b\mathcal{L}(w)(p)+\frac{\alpha b}{p}\left(\sum_{t^f\in\mathcal{F}}e^{-pt^f}-\sum_{t^r\in\mathcal{R}}e^{-pt^r}\right).$$

We obtain

$$\mathcal{L}(v)(p)=\frac{\mu p+b(\mu-\alpha)}{p(p+b)(p+\tau^{-1})}\left(\sum_{t^f\in\mathcal{F}}e^{-pt^f}-\sum_{t^r\in\mathcal{R}}e^{-pt^r}\right)+\frac{1}{p+\tau^{-1}}\mathcal{L}(I)(p).$$

Using inverse Laplace transform, we have

$$v(t)=\sum_{t^f\in\mathcal{F}}\eta(t-t^f)-\sum_{t^r\in\mathcal{R}}\eta(t-t^r)+\int_0^\infty\epsilon(s)I(t-s)ds, \tag{F1}$$

where

$$\eta(t)=\tau(\mu-\alpha)+\left(\frac{\alpha b\tau^2}{b\tau-1}-\mu\tau\right)e^{-t/\tau}-\frac{\alpha\tau}{b\tau-1}e^{-bt},$$

$$\epsilon(t)=e^{-t/\tau}.$$

Note that we do not consider the special case $b=1/\tau$.

APPENDIX G: THE PERIODIC SOLUTION OF THE PML EQUATIONS

Techniques are similar to those described for the PFN model and we summarize the main steps. Applying Fourier series on the differential formulation of the PML or, equivalently, the Poisson formula on the integral expression of the PML, we find

$$v_\infty(t)=\overline{v}_\infty+\eta_\infty(t+\zeta)-\eta_\infty(t-\zeta),$$

where

$$\overline{v}_\infty=\frac{2\zeta}{T}(1-\alpha)+I,$$

$$\eta_{\infty,n}=\frac{bT(1-\alpha)+2i\pi n}{2i\pi Tn\left(b-\frac{4\pi^2n^2}{T^2}+\frac{2i\pi n}{T}(1+b)\right)},$$

and therefore,

$$v_{\infty,n}=\eta_{\infty,n}(e^{2i\pi n\zeta/T}-e^{-2i\pi n\zeta/T})$$

and

$$v_{\infty,0}=\overline{v}_\infty.$$

We calculate

$$\eta_\infty(t)=(1-\alpha)\left(\frac{1}{2}-\frac{t}{T}\right)+\frac{b(\alpha-1)+1}{b-1}\frac{e^{-t}}{1-e^{-T}}-\frac{\alpha}{b-1}\frac{e^{-bt}}{1-e^{-bT}}$$

for $0\leqslant t\leqslant T$ and $\eta_\infty(t)$ is defined on R by periodicity. The periodic solutions are related to the existence of T and ζ that satisfy

$$v_\infty(\zeta)=v_\infty(-\zeta)=\vartheta$$

and we obtain a system of two transcendental equations

$$I-I_1+F(x,y)=0, \tag{G1}$$

$$I_2-I+F(x,x-y)=0, \tag{G2}$$

where $x=T/2$, $y=\zeta$, and

$$F(x,y)=\frac{b(\alpha-1)+1}{1-b}\frac{1-e^{-2y}}{1-e^{-2x}}+\frac{\alpha}{b-1}\frac{1-e^{-2by}}{1-e^{-2bx}}.$$

Parameters I_1, I_2 are related to the two saddle-node bifurcations. Note that there is no periodic solutions with a sliding motion since a periodic trajectory cannot meet tangentially the line of discontinuity.

For $I-I_1$ (or I_2-I) a small positive constant, one expects to find a large period value (since we are close to the saddle-node bifurcation). For $x\gg1$, we define $u=e^{-2x}$ if $b>1$ or $u=e^{-2bx}$ if $b<1$. As $u\to0$, we have

$$F(x,y)=c_1(1-e^{-2y})+c_2(1-e^{-2by})+O(u), \tag{G3}$$

where $c_1=[1+b(\alpha-1)]/(1-b)$ and $c_2=\alpha/(b-1)$. Assuming that the periodic solution spends a constant time in the superthreshold regime, that is, $y=y_0+O(u)$, we have

$$F(x,x-y)=c_1+c_2+O(u)$$

and y_0 is given canceling the right-hand side of Eq. (G3). We have $c_1+c_2=1-\alpha$ and using $I_2=I_1+\alpha-1$, the requirement (G2) leads to the necessary condition $I-I_1=O(u)$, that is, I is near the first-saddle-node bifurcation. The other situation (I close to I_2) is obtained assuming that the duration of the superthreshold regime y and the period x have the same order, that is, $x-y=y_0+O(u)$.

For $I-I_1=O(u)$, we find

$$I-I_1=\kappa u, \tag{G4}$$

where κ is a constant obtained canceling the leading order expansion of F. Using $u=e^{-T}$ (for $b>1$), we find

$$T\sim-\ln(I-I_1).$$

Note that the symmetrical situation (I close to I_2) leads to a similar logarithmic law. When $b<1$, we have

$$T\sim-\frac{1}{b}\ln(I-I_1).$$

APPENDIX H: THE INTEGRATE-AND-FIRE MODEL WITH A SPIKE DESCRIPTION

1. Integral formulation of the IFS

The IFS model with the same relaxation time in the subthreshold and superthreshold regime is given by

$$\frac{dv(t)}{dt}=-\frac{v(t)}{\tau}+\mu h[v(t)-\vartheta]+I_e(t),$$

$$v(t)=\vartheta^{\text{peak}}\Rightarrow v(t^+)=v_r.$$

Note that the threshold process can be generalized to non-continuous threshold crossings. First, we introduce the reset conditions as reset currents

$$\frac{dv(t)}{dt}=-\frac{v(t)}{\tau}+\mu h[v(t)-\vartheta]-(\vartheta^{\text{peak}}-v_r)\times\sum_{t^r\in\mathcal{R}}\delta(t-t^r)+I_e(t). \tag{H1}$$

Using the definition of t^f and t^r, we have

$$h[v(t)-\vartheta]=\sum_{t^f\in\mathcal{F}}h(t-t^f)-\sum_{t^r\in\mathcal{R}}h(t-t^r), \tag{H2}$$

where we assume that each firing time t^f is related to a reset time t^r. In other words, the return to the subthreshold regime is not due to the current $I_e(t)$. This assumption holds when c_2 is small or μ is large.

Using (H2), we transform (H1) into a linear nonautonomous differential equation

$$\frac{dv(t)}{dt}=-\frac{v(t)}{\tau}+\mu\sum_{t^f\in\mathcal{F}}h(t-t^f)-\mu\sum_{t^r\in\mathcal{R}}h(t-t^r)-(\vartheta^{\text{peak}}-v_r)\sum_{t^r\in\mathcal{R}}\delta(t-t^r)+I_e(t).$$

As an initial condition, we take $v(0)=0$. The integration yields

$$v(t)=\mu\sum_{t^f\in\mathcal{F}}\int_0^\infty h(t-t^f-s)e^{-s/\tau}ds-\mu\times\sum_{t^r\in\mathcal{R}}\int_0^\infty h(t-t^r-s)e^{-s/\tau}ds-(\vartheta^{\text{peak}}-v_r)\times\sum_{t^r\in\mathcal{R}}\int_0^\infty\delta(t-t^r-s)e^{-s/\tau}ds+\int_0^\infty e^{-s/\tau}I_e(t-s)ds,$$

which gives

$$v(t)=\mu\tau\sum_{t^f\in\mathcal{F}}(1-e^{-(t-t^f)/\tau})-\mu\tau\sum_{t^r\in\mathcal{R}}(1-e^{-(t-t^r)/\tau})-(\vartheta^{\text{peak}}-v_r)\sum_{t^r\in\mathcal{R}}e^{-(t-t^r)/\tau}+\int_0^\infty e^{-s/\tau}I_e(t-s)ds.$$

We thus obtain

$$v(t)=\sum_{t^f\in\mathcal{F}}\eta_f(t-t^f)-\sum_{t^r\in\mathcal{R}}\eta_r(t-t^r)+\int_0^\infty\epsilon(s)I(t-s)ds,$$

where for $t\geqslant 0$,

$$\eta_f(t)=\mu\tau(1-e^{-t/\tau}),\qquad \eta_r(t)=(\vartheta^{\text{peak}}-v_r)e^{-t/\tau}+\mu\tau(1-e^{-t/\tau}),\qquad \epsilon(t)=e^{-t/\tau}, \tag{H3}$$

and 0 otherwise. Just as for the standard IF model, the IFS model has a resetting kernel, $\eta_r(t-t^r)$, related to the reset process. However, the IFS model provides an explicit form of the action potential, $\eta_f(t-t^f)$, whereas in Eq. (7) action potentials where reduced to a point in time.

2. Relations with the two-dimensional models

The relations between the IFS model and the two-dimensional models are simply illustrated considering a slow recovery process, i.e., small values of b, in Eqs. (12) and (21). Using the integral formulation of the PFN or PML models, we calculate the leading order expansion of the two kernels

$$\eta_0(t)=\mu\tau(1-e^{-t/\tau}),\qquad \epsilon_0(t)=e^{-t/\tau}. \tag{H4}$$

The zero order approximation reveals the similarity with the expressions of the IFS kernels [see Eq. (H3)]. Unfortunately, the zero-order terms are not sufficient to account for recovery in the two-dimensional systems. When tb is $O(1)$ order, expansion (H4) becomes nonuniform and we have to consider the different terms tb in the expansion of η. We enter in a new phase where the smooth recovery process operates.

[1] W.M. Yamada, C. Koch, and P.R. Adams, in *Methods in Neuronal Modeling: From Ions to Networks*, 2nd ed., edited by C. Koch and I. Segev (MIT Press, Cambridge, MA, 1998), pp. 137–170.

[2] M.A. Wilson, U.S. Bhalla, J.D. Uhley, and J.M. Brower, in *Advances in Neuronal Information Processing Systems*, edited by D. Touretzky (Morgan Kaufmann, San Mateo, CA, 1989), pp. 485–492.

[3] L. Lapicque, J. Physiol. Pathol. Gen. **9**, 620 (1907).

[4] L.F. Abbott and C. van Vreeswijk, Phys. Rev. E **48**, 1483 (1993).

[5] W. Maass and C.M. Bishop, *Pulsed Neural Networks* (MIT Press, Cambridge, 1999).

[6] A.F. FitzHugh, Biophys. J. **1**, 445 (1961).

[7] J. Nagumo, S. Arimoto, and S. Oshizawa, Proc. IRE **50**, 2061 (1962).

[8] L. Morris and H. Lecar, Biophys. J. **35**, 193 (1981).

[9] J.L. Hindmarsh and R.M. Rose, Nature (London) **296**, 162 (1982).

[10] J. Rinzel, Fed. Proc. **44**, 2944 (1985).

[11] L.F. Abbott and T.B. Kepler, in *Statistical Mechanics of Neural Networks*, edited by L. Garrido (Springer-Verlag, Berlin, 1990).

[12] J. Rinzel and G.B. Ermentrout, in *Methods in Neuronal Mod-*

eling: From Ions to Networks, 2nd ed., edited by C. Koch and I. Segev (MIT Press, Cambridge, MA, 1998), pp. 251–291.
[13] F.C. Hoppensteadt and E.M. Izhikevich, *Weakly Connected Neural Networks* (Springer-Verlag, New York, 1997).
[14] E.M. Izhikevich, Int. J. Bifurcation Chaos Appl. Sci. Eng. **10**, 1171 (2000).
[15] A.L. Hodgkin, J. Physiol. (London) **107**, 165 (1948).
[16] G.B. Ermentrout, Neural Comput. 8, 979 (1996).
[17] W. Gerstner, in *The Handbook of Biological Physics*, edited by F. Moss and S. Gielen (Elsevier Science, Amsterdam, 2001), Vol 4, pp. 469–516.
[18] W. Gerstner and J.L. van Hemmen, Neural Networks **3**, 139 (1992).
[19] H.P. McKean, Adv. Math. **4**, 209 (1970).
[20] A.F. Filippov, *Differential Equations with Discontinuous Right-Hand Sides* (Kluwer Academic, Dordrecht, 1988).
[21] J.P. Aubin and A. Cellina, *Differential Inclusions* (Springer-Verlag, Berlin, New York, 1984).
[22] F. Giannakopoulos and K. Pliete, Nonlinearity **14**, 1611 (2001).
[23] A. Tonnelier, SIAM (Soc. Ind. Appl. Math.) J. Appl. Math. **63**, 459 (2002).
[24] R.R. Llinas, Science **242**, 1654 (1988).
[25] A.L. Hodgkin and A.F. Huxley, J. Physiol. (London) **117**, 500 (1952).
[26] E.M. Izhikevich, Neural Networks **14**, 883 (2001).
[27] One can easily generalize the definitions of the two sets for noncontinuous dynamics of the membrane potential.
[28] Note that the leaky integrator neuron presents a resonant behavior when $b>0$.
[29] The case $\gamma=0$ is not interesting since a rescaling of w allows to set $I=0$.
[30] An additional bifurcation occurs for a particular range of γ values (not shown in Fig. 7). This bifurcation is a double homoclinic bifurcation which appears when the two unstable periodic solutions with sliding motion bifurcates from an unstable periodic solution. These two unstable limit cycles surround the two fixed points, respectively, and become simultaneously homoclinic to a degenerate saddle point along the line of discontinuity (as the bifurcation point is reached). We do not analyze this situation since unstable cycles are not directly observable.
[31] A.R. Bulsara, R.D. Boss, and E.W. Jacobs, Biol. Cybern. **61**, 211 (1989).
[32] X. Chen and S.P. Hastings, J. Math. Biol. **38**, 1 (1999).
[33] S.H. Strogatz, *Nonlinear Dynamics and Chaos. With Application to Physics, Biology, Chemistry and Engineering* (Addison-Wesley, Reading, MA, 1994).
[34] H.G. Othmer and M. Xie, J. Math. Biol. **39**, 139 (1999).
[35] S. Coombes, Physica D **2820**, 1 (2001).
[36] W.M. Kistler, W. Gerstner, and J.L. van Hemmen, Neural Comput. **9**, 1015 (1997).